Rev. Mexicana Astron. Astrof., **22**, 265-273 (1991)

MODELS OF SPATIALLY RESOLVED RECOMBINATION REGIONS IN H-H OBJECTS

A.C. Raga[1] and L. Binette

Canadian Institute for Theoretical Astrophysics, Canada

Received 1991 April 18

RESUMEN

Algunos objetos Herbig-Haro (H-H) aparentemente son el resultado de "choques a proa" alrededor de las "cabezas" de jets (chorros) estelares. Observaciones recientes de dos de estos objetos (HH 34 y HH 111) muestran que las alas de los choques a proa tienen una estructura estratificada, con la emisión en [S II] localizada detrás de la emisión en Hα (en otras palabras, la emisión en Hα tiene un máximo localizado más lejos de la fuente que el máximo de la emisión en [S II]). Las separaciones angulares Hα/[S II] observadas están en el rango de 0.4"-1.4", correspondiendo a separaciones espaciales de 2 a 9 $\times$ 10^{15} cm.

En este artículo, discutimos si estos resultados se pueden o no interpretar como evidencia de que la zona de recombinación detrás de los choques a proa esté resuelta espacialmente en las observaciones. Encontramos que las separaciones angulares entre la emisión de Hα y de [S II] en efecto probablemente sean el resultado de la estratificación post-choque, la cual resulta ser observable debido a la baja densidad prechoque de estos objetos ($n_H \sim 10$ cm^3 en HH 34 y HH 111) y a la baja velocidad de choque ($\sim 30-50$ km s^{-1}) de las alas de los choques a proa. De nuestros modelos tambien obtenemos predicciones de las separaciones espaciales entre Hα y las lineas de [O I] y [O II]. Observaciones futuras de estas lineas de emisión podrían ayudar a confirmar la posible validez de nuestros modelos.

ABSTRACT

A few Herbig-Haro (H-H) objects appear to correspond to bowshocks which might be formed at the heads of jet-like flows. Recent observations show that for two of these objects (HH 34 and HH 111) the bowshock wings have a stratified structure, with the [S II] emission "trailing" the Hα emission (i. e., the Hα emission is observed to peak farther away from the source than the [S II] emission). The observed Hα/[S II] angular offsets are in the 0.4"-1.4" range, corresponding to physical separations of (2-9) $\times$ 10^{15} cm.

In this paper, we study whether or not these observed offsets can be interpreted as evidence that the recombination regions behind the bowshocks are spatially resolved in the observations. We find that the observed Hα/[S II] offsets indeed probably are the result of the postshock stratification, which is observable because of the low preshock density for these objects ($n_H \sim 10$ cm^3 for HH 34 and HH 111) and the low shock velocity ($\sim 30-50$ km s^{-1}) of the bowshock wings. From our models, we also obtain predictions for the spatial offsets that should be observed between Hα and the [O I] and [O II] lines. Future observations of such offsets would help to confirm our models.

Key words: **HERBIG HARO OBJECTS – HYDRODYNAMICS**

INTRODUCTION

It is now quite generally accepted that at least part of the emission of Herbig-Haro (H-H) objects is produced in the recombination region of shock waves (as first suggested by Schwartz 1975). This conclusion has been reached to a large extent as a result of the good qualitative agreement between the line ratios observed in H-H spectra (e. g., Brugel, Böhm and Mannery 1981) and the predictions from plane-parallel shock wave models (e. g., Raymond 1979, Dopita 1978).

However, one of the most interesting predictions

1. Present address: University of Manchester, England.

of shock wave models is the existence of a clear stratification, with the hotter, higher excitation and ionization gas close to the shock wave, and cooler, more neutral gas farther downstream (i. e., at larger distances from the shock wave). Let us summarize the observational evidence for such a stratification:

1. Schwartz (1981) observed a correlation between radial velocity and excitation for spectral lines in HH 1 and 2.

2. Solf, Böhm and Raga (1988) carried out empirical electron temperature determinations (from temperature sensitive forbidden line ratios) for a number of ions, and found that the temperature monotonically increases for increasing ionization potential of the ions.

Both of these effects can be interpreted as a direct consequence of the stratification of the recombination region behind a shock wave. However, other geometric effects (e. g., the presence of strongly curved shock waves) might in principle have similar observational consequences, so that these results cannot be interpreted as uncontroversial evidence for the existence of a stratified recombination region.

Shock waves in H-H objects are likely to be strongly curved (a direct result of their small size). Also, at any given position in an H-H object one might be observing the emission from more than one shock wave (see, e. g., Hartigan 1989). These facts make it quite difficult to disentangle the observational evidence for post-shock stratification from the other geometric effects which are also present.

The ideal situation would be to look at a region of an H-H object where the emission is produced by a single, not strongly curved shock wave. Models of stellar jets (which are successful at reproducing the observations of some H-H objects) suggest that the wings of the bowshock at the head of the jet have the required characteristics (Blondin, Fryxell and Königl 1990). For appropriate model parameters, bowshocks with extended emitting wings are produced (Raga 1988). The emission in these bowshock wings is produced exclusively as a result of the heating and compression in the slowly curving bowshock.

From this, we would conclude that H-H objects which show a bowshock morphology are very good candidates for direct observations of the post-shock stratification. In fact, CCD images of the very striking bowshock structures of HH 34 (Bührke, Mundt and Ray 1988) and HH 111 (condensation V, Reipurth 1989a; Reipurth, Raga and Heathcote 1991) show spatial offsets between the Hα and [S II] 6717+6731 bowshock wings (with the [S II] wing "trailing" the Hα wing). As Bührke *et al.* (1988) have pointed out, this can be interpreted as being a direct observation of the stratification in the recombination region behind the bowshock. If this interpretation is indeed correct, this would constitute the most clear and direct observational evidence for the presence of a recombination region.

In the present paper, we discuss predictions of spatial offsets between different emission lines from 1-D numerical shock models. We also derive analytic scaling laws that reproduce the numerical results, and are useful for carrying out comparisons with observations.

II. OBSERVATIONAL MOTIVATION

The HH 34 and HH 111 outflows show H-H objects (HH 34S and HH 111V, respectively) with a very striking bowshock morphology. These bowshock structures show the following interesting property. From an analysis of Hα and [S II] (6717+6731) narrow-band CCD images, Bührke *et al.* (1988) noted the existence of a displacement between the Hα and [S II] wings of the HH 34S bowshock. The [S II] emission is seen to be "trailing" the Hα emission (i. e., the Hα intensity peaks farther away from the source than the [S II] emission). The offset between the Hα and [S II] bowshock wings has values between 1" and 1.4", corresponding to a physical separation in the range of $(7\text{-}9)\times10^{15}$ cm (at a distance of 450 pc). A similar effect is observed in the HH 111V bowshock (Reipurth, Raga and Heathcote 1991), where the [S II] bowshock wing is observed to be trailing the Hα wing with spatial offsets in the $(2.4\text{-}3.8)\times10^{15}$ cm range.

Bührke *et al.* (1988) noted that such offsets could represent a direct observation of the stratification in the recombination region behind the bowshock. In the following sections, we present models which illustrate for which parameters such offsets are indeed obtained.

III. NUMERICAL MODELS

We model the recombination region behind the wings of a bowshock as a simple, steady 1-D flow. This approximation to the much more complex 2-D problem is valid provided that the cooling distance is much smaller than the radius of curvature of the bowshock. As we are trying to reproduce the observations described in §II (of $\sim 1'$ cooling regions in bowshocks with $\sim 10"$ radii), this condition is satisfied at least in an approximate way.

The properties of the recombination region are mainly determined by the shock velocity V_S (i. e., the component of the bowshock velocity normal to the shock), and the preshock density n_H (the hydrogen number density of the undisturbed gas ahead of the bowshock). Provided that the collisionally excited line cooling is in the low density regime (i. e., that collisional de-excitation processes

lo not play an important role), the preshock lensity n_H enters the solution as a simple scaling $d \propto n_H^{-1}$) of the depth of the recombination egion. This scaling with preshock density is not atisfied exactly by models with $n_H > 10$ cm^{-3} though this value actually depends on the shock elocity V_S). In high density models, the postshock lectron density is large enough for collisional de-xcitation processes to start playing an important ole. However, the effect of such processes on he size of the recombination region is not very ramatic, so that for the purpose of this paper we an assume that the $d \propto n_H^{-1}$ scaling holds in an pproximate way throughout the preshock density ange that we have studied.

A factor that complicates the choice of model pa-ameters is the strong dependence of the postshock mission on the ionization state of the preshock gas in particular, on the ionization state of hydrogen). The ionization state of the preshock gas in principle s determined in a self-consistent way by the preio-ization that results from the ionizing photons pro-uced in the recombination region. However, time-lependent effects (which would lower the preioni-ation; Innes, Giddings and Falle 1987) and the omplex geometry of the bowshock (which would end to increase the preionization in the bowshock vings; Raymond, Hartigan and Hartmann 1988) nake it impossible to calculate the preionization in erms of steady, 1-D shock models. Because of this, ve have considered the ionization fraction of hydro-gen in the preshock gas (x_{HII}) as a free parameter of our models. We have assumed that helium is neutral in the preshock gas, except for the case of the models with $x_{HII} = 0.9$ (see below), in which helium is taken to be 30 % singly ionized. Furthermore, we have considered all of the other elements to be neutral, except for sulphur and carbon, which we assume are singly ionized. Also, because we have restricted our study to strong shocks, the value of the preshock temperature does not affect very strongly the structure of the recombination region (we have chosen a preshock temperature of 10^4 K for all of our models).

The shock wave models have been computed with the MAPPINGS code, in which a large number of atomic processes are considered (see, e. g., Binette, Dopita and Tuohy 1985). Solar abundances have been assumed. In Figure 1, we show the emission coefficients of the Hα, [O II] (3726+29), [O I] (6300) and [S II] (6717+31) lines as a function of y (the distance from the shock wave). Actually, the x-axis is $y \times n_H$ (where n_H is the preshock hydrogen number density), so that the distance y can be obtained in a straightforward way for any value chosen for n_H.

We have chosen these particular spectral lines for our study because they are observed to be strong in low excitation H-H objects (see, e g., Brugel *et al.* 1981). Also, previous calculations of shock wave models (e. g., Hartigan, Raymond and Hartmann 1987) show that these lines are strong for shock

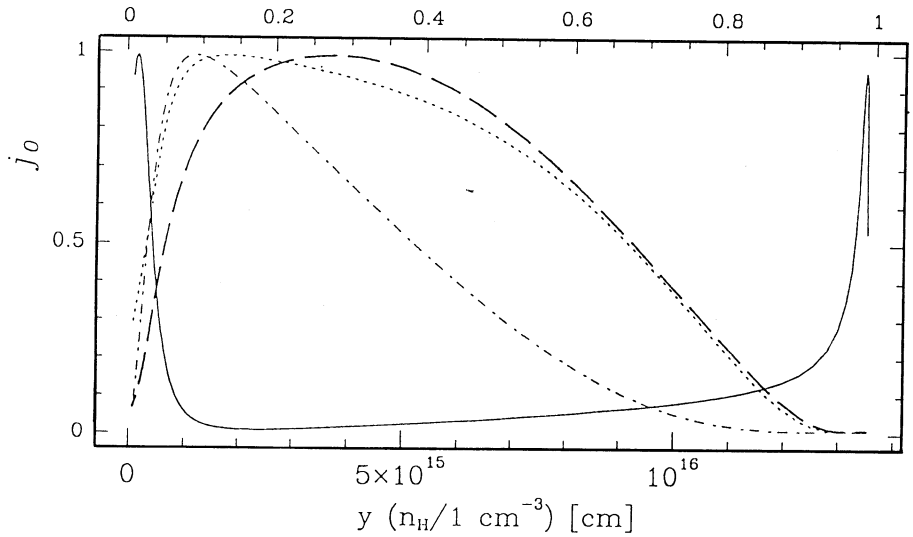

ig. 1. The Hα (solid line), [O II] 3726+29 (dot-dash line), [O I] 6300 (dotted line) and [S II] 6717+31 emission oefficients as a function of distance y from the shock wave. The emission coefficients are normalized so that the peak alues are equal to 1. The results shown correspond to a 52 km s^{-1} shock wave moving into a medium with 50% reionized hydrogen (see the text). The scaling of the recombination region with preshock (hydrogen) number density $_H$ is given in the x-axis label.

waves in the 30-80 km s^{-1}velocity range (in which we are interested, see below).

The results shown in Figure 1 correspond to a model with shock velocity V_S = 52 km s^{-1}, and a hydrogen preionization fraction x_{HII} = 0.5. The following interesting result is obtained. While the [O II], [O I] and [S II] emission coefficients show a spatial dependence with a well defined maximum (i. e., the emission coefficients first grow, then peak, and eventually decrease for increasing distances y from the shock), the Hα emission coefficient shows two maxima. The Hα maximum close to the shock wave (at $y \approx 2 \times 10^{14}$ cm, see Figure 1) is a result of collisional excitation in the hot postshock region, where the neutral hydrogen atoms are rapidly being ionized. The second Hα maximum (at $y \approx 1.35 \times 10^{15}$ cm, see Figure 1) corresponds to the emission from the recombination cascade of hydrogen ions that are recombining in the cooler regions farther away from the shock.

It is clear from Figure 1 that the two Hα emitting regions (the "collisional excitation" and "recombination" regions, see above) produce roughly comparable intensities. If we lower the hydrogen preionization fraction (x_{HII} = 0.5 for the model shown in Figure 1, see above), the collisional excitation Hα peak gains in relative intensity. On the other hand, if hydrogen is fully preionized (x_{HII} = 1), the collisional excitation peak is simply not present.

From this, we see right away that if we want to reproduce observations in which a [S II] bowshock wing is seen to be "trailing" the Hα emission, we have to consider models with low preionization fractions. For models with x_{HII} > 0.5, the Hα emission is dominated by the recombination component, which peaks farther away from the source than the [S II] emission (see above and Figure 1), so that the observed [S II]-Hα position offset would be opposite to what is observed. The existence of this effect was already noted by Bührke *et al.* (1988).

In Figure 2, we show the distances $d_{[O\ II]}$, $d_{[O\ I]}$ and $d_{[S\ II]}$ between the position of the collisional excitation Hα intensity peak and the intensity peaks of the [O II] (3726+29), [O I] (6300) and [S II] (6717+31) emission lines (also see Figure 1). The positions of the emission line intensity peaks (used for determining these spatial line offsets) correspond to the positions of the maximum values of the corresponding line emission coefficients. However, as is clear from Figure 1, the behaviour of the emission coefficients as a function of distance from the shock is considerably different for the different emission lines (for example, the [O II] lines show a much sharper spatial peak than the [S II] lines).

For shocks with low preionization (x_{HII} < 0.5, see above), the distances $d_{[O\ II]}$, $d_{[O\ I]}$ and $d_{[S\ II]}$ correspond to the [O II]-Hα, [O I]-Hα and [S II]-Hα offsets that would be observed in a bowshock wing (the offsets are a strong function of the flow velocity V_S perpendicular to the shock wave, see Figure 2). However, if the preionization is higher, the Hα emission would be dominated by the recombination component, and the distances given in Figure 2 would not correspond to the observed offsets.

We have carried out predictions of $d_{[O\ II]}$, $d_{[O\ I]}$ and $d_{[S\ II]}$ (see above) for models with shock velocities in the 38-78 km s^{-1} range, and hydrogen preionization fractions x_{HII} = 0.01, 0.5, 0.5 and 0.9. The predictions from the models with x_{HII} = 0.9 are mostly only of academic interest, since for these models the Hα emission is dominated by the recombination contribution (see above and Figure 1), so that the predicted $d_{[O\ II]}$, $d_{[O\ I]}$ and $d_{[S\ II]}$ values do not correspond to directly observable quantities. In the following section, we present an interpretation of these results.

IV. ANALYTIC SCALING LAWS

Let us now consider the following problem. We have already discussed how the depth d of the recombination region scales with the preshock (hydrogen) density n_H. Is it also possible to derive a simple scaling law for d as a function of the shock velocity V_S ? This can be done as follows.

For a strong shock in a pure hydrogen, neutral gas, the postshock temperature T is approximately given by:

$$T = \frac{3}{16}\frac{m_H V_S^2}{k}, \qquad (1)$$

where V_S is the shock velocity, m_H is the mass of the hydrogen atom, and k is Boltzmann's constant. The thermal energy of the postshock gas will then be radiated away in a timescale τ_{cool} approximately given by :

$$\tau_{cool} \approx \frac{(3/2)\, n_{H,1} kT}{n_{H,1}^2\, \Lambda(T)} \qquad (2)$$

where $n_{H,1}^2\, \Lambda(T)$ is the (radiative+collisional ionization) cooling rate (per unit volume and time) and $n_{H,1}$ is the postshock hydrogen number density ($\approx 4 n_H$, because for a strong shock the compression has a value of approximately 4). The cooling distance d_{cool} is proportional to the product $\tau_{cool} V_S$, so that from equations 2 and 3, we obtain:

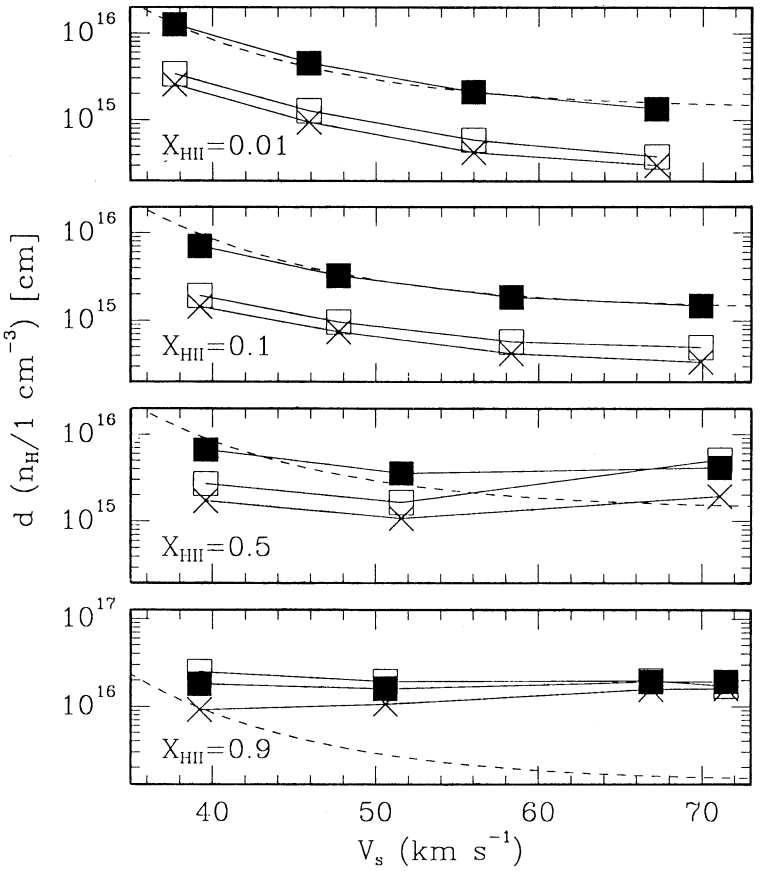

Fig. 2. Spatial offsets between the collisionally excited Hα emission peak and the [O II] 3726+29 (crosses), [O I] 6300 (open squares) and [S II] 6717+31 (solid squares) emission line maxima ($d_{[O\ II]}$, $d_{[O\ I]}$ and $d_{[S\ II]}$, respectively). The offsets obtained from numerical shock wave models with hydrogen preionization fractions X_{HII} = 0.01, 0.1, 0.5 and 0.9 are given as a function of shock velocity V_S. The dashed curves represent the $d_{[S\ II]}$ vs. V_S dependence obtained from the analytic scaling law (described in the text).

$$d_{cool} \propto \frac{V_S\, T}{n_H\, \Lambda(T)} \ . \qquad (3)$$

This equation shows the distance/preshock density scaling law described in §III. It also shows that the dependence of d_{cool} on the shock velocity V_S comes through the temperature dependence of the cooling function $\Lambda(T)$ (where the postshock temperature T is determined by V_S, see equation 1). To make further progress, we have to specify what is the function $\Lambda(T)$. This can be done in the following way.

If the preshock gas is neutral, we speculate that the postshock cooling for shock waves with V_S = 30–80 km s^{-1}is dominated by the collisional ionization of hydrogen. Under this assumption, we would conclude that $\Lambda(T)$ is proportional to the collisional ionization coefficient of hydrogen:

$$\Lambda(T) = C\, T^{1/2} \exp\left(-\frac{\chi_H}{kT}\right) , \qquad (4)$$

where χ_H is the ionization potential of hydrogen, and C is a constant (see Cox 1970). From equations 1, 3 and 4, we then obtain :

$$d_{cool} \propto \frac{{V_S}^2}{n_H} \exp\left(\frac{6950}{{V_S}^2}\right) , \qquad (5)$$

where V_S is in km s^{-1}, and we have substituted the numerial values for the atomic constants. In logarithmic form, we have:

$$\log_{10}\left(\frac{d_{cool}\, n_H}{{V_S}^2}\right) = const. + \frac{3020}{{V_S}^2}\,. \qquad (6)$$

With our numerical shock models, it is easy to check whether or not this scaling law is correct. In Figure 3, we plot $\log_{10}(d\, n_H/{V_S}^2)$ as a function of ${V_S}^{-2}$ (with V_S in km s^{-1}) for the models described in §III (see also Figure 2). The distances $d_{[O\ II]}$, $d_{[O\ I]}$ and $d_{[S\ II]}$ are the offsets between the maxima of the [O II], [O I] and [S II] emission and the collisionally excited Hα component (see Figures 2 and 3).

From Figure 3, it is clear that for the models with hydrogen preionization fractions $X_{HII} = 0.01$ and 0.1 we do obtain a $\log_{10}(d\, n_H/{V_S}^2) \propto {V_S}^{-2}$ dependence. From linear fits to the three emission line offsets ($d_{[O\ II]}$, $d_{[O\ I]}$ and $d_{[S\ II]}$), we obtain a proportionality constant with a value of 2920 (approximately the same number is obtained for the three emission line offsets), in surprisingly good agreement with the value (3020, see equation 6) obtained from our simple analytical considerations.

In Figure 3, we also see that this simple scaling law starts to break down for the $x_{HII} = 0.5$ models, and that the $x_{HII} = 0.9$ models show a very different distance vs. velocity dependence. This lack of agreement between the numerical models and the analytic scaling law is not surprising, as for deriving this scaling law we have assumed that the cooling rate is dominated by the collisional io-

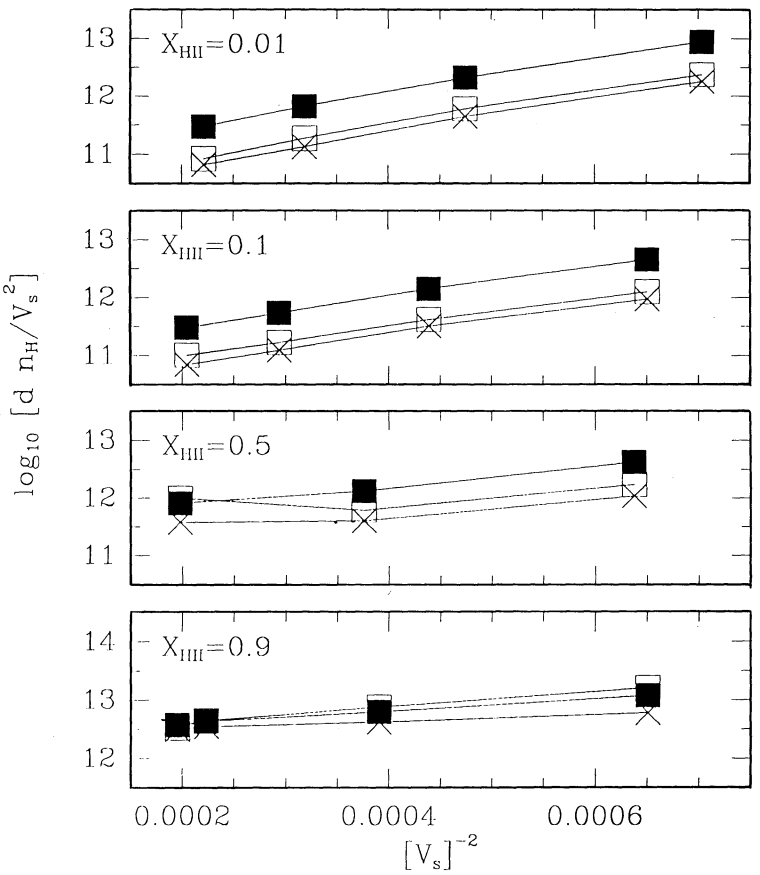

Fig. 3. This figure shows the same results as Figure 2, but plotted as $\log_{10}[d\, n_H/{V_S}^2]$ vs. $[{V_S}^{-2}]$ (with d in cm, n_H in cm^3 and V_S in km s^{-1}). The results with $d = d_{[O\ II]}$, $d_{[O\ I]}$ and $d_{[S\ II]}$ are plotted with crosses, open squares and solid squares, respectively. The results for shock wave models with hydrogen preionization fractions $X_{HII} = 0.01$, 0.1, 0.5 and 0.9 are shown.

nization of hydrogen (and this will definitely not be true for models with high hydrogen preionization fractions). However, as we have mentioned above, in this paper we are interested in low preionization models (in which the Hα emission is dominated by the collisional excitation component located immediately downstream of the shock, see Figure 1), so that the analytic scaling law we have derived above is indeed applicable.

From linear fits to the $\log_{10}(d\, n_H/V_S{}^2)$ vs. $V_S{}^{-2}$ dependences obtained from the $x_{HII} = 0.01$ models (see Figure 3), we obtain:

$$d_{[O\ II]} = \left(1.60 \times 10^{10}\ \mathrm{cm}\right) \times \left(n_H\, 10^{2920/V_S{}^2}\right), \quad (7)$$

$$d_{[O\ I]} = \left(2.21 \times 10^{10}\ \mathrm{cm}\right) \times \left(n_H\, 10^{2920/V_S{}^2}\right), \quad (8)$$

$$d_{[S\ II]} = \left(7.89 \times 10^{10}\ \mathrm{cm}\right) \times \left(n_H\, 10^{2920/V_S{}^2}\right), \quad (9)$$

where the preshock hydrogen number density n_H is in cm^{-3} and V_S in $\mathrm{km\ s}^{-1}$. The values obtained for $d_{[S\ II]}$ from equation 9 are plotted in Figure 2, showing the good agreement that we find between our d vs. V_S scaling law and the predictions from the numerical models.

These analytic expressions for the emission line spatial offsets can be used to define constant-offset contours in the (V_S, n_H) plane. In Figure 4, we show contours of constant [S II]-Hα offsets ($d_{[S\ II]}$, see equation 9) for a range of shock velocities and preshock densities. Such "diagnostic diagrams" can be most easily constructed from equations 7-9, and are useful for comparisons with observational results.

In the following section, we present a comparison of these predictions with the observations of HH 34 and HH 111 which we have described in §II.

V. COMPARISON WITH OBSERVATIONS OF HH 34 AND HH 111

In §II, we have discussed observations of bowshock structures in HH 34 (Bührke *et al.* 1988) and HH 111 (Reipurth *et al.* 1991). The HH 34 observations show Hα-[S II] offsets of (7-9)×10^{15} cm in the bowshock wings. The HH 111 observations show offsets of (2.4-3.8)×10^{15} cm (see §II). We can use these results to evaluate for what (V_S, n_H) values the observed offsets would correspond to our predictions.

The Hα-[S II] offset values observed for HH 34 and for HH 111 can be used to determine the

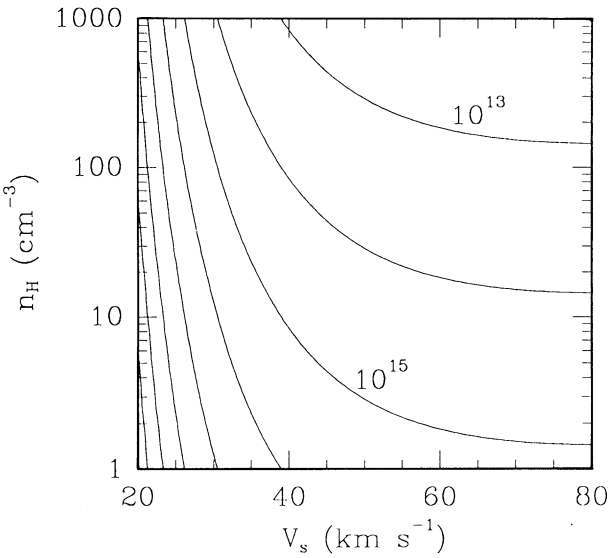

Fig. 4. Constant-$d_{[S\ II]}$ contours in the (V_S, n_H) plane (where V_S is the shock velocity, and n_H is the preshock hydrogen number density) obtained from the analytic expression for the Hα-[S II] 6717+31 offset. Two successive contours correspond to a ratio of 10 in $d_{[S\ II]}$ (the values of two of the contours, 10^{13} cm and 10^{15} cm are indicated in the graph).

possible range of shock velocities and preshock densities for both H-H objects. This is shown in Figure 5, where we have used the range of offsets observed for each H-H object in order to derive the (V_S, n_H) values that would produce such offsets (using equation 9).

Bührke *et al.* (1988) have estimated that the HH 34S bowshock is moving into a medium with a preshock density $n_H \approx$ 5-10 cm^{-3}. From Figure 5, we see that the observed Hα-[S II] offsets would then imply a shock velocity (i. e., the velocity of the bowshock normal to the bowshock surface) $V_S \sim$ 32 $\mathrm{km\ s}^{-1}$.

The observations of HH 111 of Reipurth (1989a) show that the electron density of the HH 111V bowshock is roughly comparable to the electron density of HH 34S. Given the fact that both these two bowshocks also have low radial velocities and very similar proper motions (Reipurth 1989b; Reipurth *et al.* 1991), we would conclude that the preshock density for the HH 111V bowshock also has a value $n_H \sim 10\ \mathrm{cm}^{-3}$. From Figure 5, we see that the observed Hα-[S II] offset would then imply a shock velocity $V_S \sim 35\ \mathrm{km\ s}^{-1}$ (only slightly higher than the value obtained for HH 34S).

In this comparison between observations and model predictions we have assumed that the HH 34 and HH 111 flows are in the plane of the sky, so

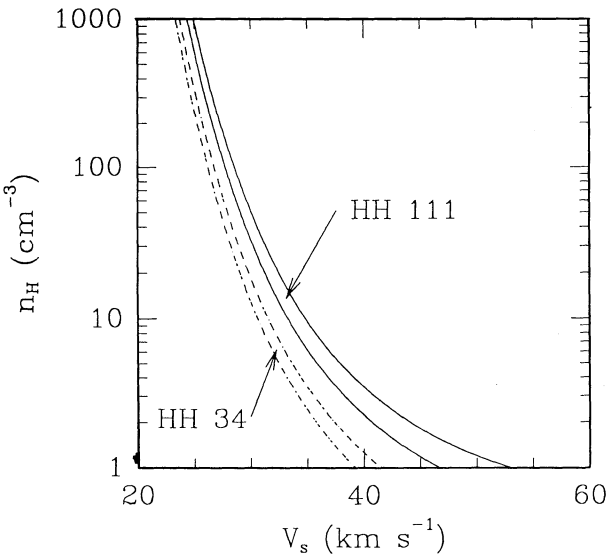

Fig. 5. n_H vs. V_S plot (where n_H is the preshock hydrogen number density, and V_S is the shock velocity) in which we show the parameter ranges that are necessary for reproducing the Hα-[S II] 6717+31 offsets (i.e., the $d_{[S\ II]}$ values) observed in the bowshock wings of HH 34S and HH 111V. The area enclosed by the two dashed lines encompasses the range of (V_S, n_H) that produces the values of $d_{[S\ II]}$ observed in HH 34. The area enclosed by the two solid lines encompasses the range of (V_S, n_H) that produces the values of $d_{[S\ II]}$ observed in HH 111.

that we have not carried out any corrections for projection effects. However, such effects are likely to be small for the case of HH 34 and HH 111, because their large proper motions and low radial velocities imply that the axes of these outflows are indeed very close to the plane of the sky (Reipurth *et al.* 1986; Reipurth 1989b; Reipurth *et al.* 1991).

We should note that the interpretation of the Hα-[S II] offsets in the HH 34 and HH 111 bowshock wings as resolved recombination regions has the following interesting implication. If this interpretation is correct, the observed Hα emission would be formed immediately downstream of the shock. This region is potentially quite hot, which implies a quite considerable Doppler broadening of the Hα emission (the Doppler width would be comparable to the shock velocity). In the future, detailed comparisons between high resolution spectroscopic observations and theoretical models should be able to show whether or not such an effect is present.

VI. CONCLUSIONS

We have presented results from numerical models of 1-D shocks for several different shock velocities and hydrogen preionization fractions. We have used these models to calibrate analytic scaling laws that give the Hα-[O II] 3726+29, Hα-[O I] 6300 and Hα-[S II] 6717+31 spatial offsets as a function of shock velocity V_S and preshock hydrogen number density n_H.

These results can be used to evaluate whether or not the Hα-[S II] offsets observed in the HH 34 and HH 111 bowshock wings could be interpreted as being a direct observation of a spatially resolved recombination region. We find that for the estimated preshock density of $n_H \sim 10$ cm^{-3}, these observations would agree with the model predictions provided that the shock velocity is $V_S \sim 35$ km s^{-1}. This velocity appears to be quite well defined due to the very strong dependence of the Hα-[S II] offset on V_S.

Other effects not considered in our models (e. g., the presence of magnetic fields) could also affect the predicted Hα-[S II] offsets. Because of this, our determinations of emission line offsets and our comparisons with observations have to be taken with some caution.

We tentatively conclude that the observations of HH 34 and HH 111 indeed possibly correspond to the direct spatial resolution of shock wave recombination regions. This result could be confirmed with future observational measurements of Hα-[O II] and Hα-[O I] offsets. If such observations would also agree with the model predictions presented in this paper, the case for a spatially resolved recombination region would be considerably strengthened.

A.R. and L.B. acknowledge the support of the Natural Sciences and Engineering Research Council of Canada. A. R. would like to thank B. Reipurth, S. Heathcote, J. Cantó and D. Schwartz for helpful discussions about this work. We would also like to thank an anonymous referee for pointing out that our models imply an anomalously large Hα linewidth.

REFERENCES

Binette, L., Dopita, M.A., and Tuohy, I.R. 1985, *Ap. J.*, **297**, 476.
Blondin, J.M., Fryxell, B.A., and Königl, A. 1990, *Ap. J.*, **360**, 370.
Brugel, E.W., Böhm, K.H., and Mannery, E. 1981, *Ap. J. Suppl.*, **47**, 117.
Bührke, T., Mundt, R., and Ray, T.P. 1988, *Astr. and Ap.*, **200**, 99.
Cox, D. P. 1970, Ph. D. Thesis (University of California, San Diego).
Dopita, M.A. 1978, *Ap. J. Suppl.*, **37**, 117.
Hartigan, P. 1989, *Ap. J.*, **339**, 987.
Hartigan, P., Raymond, J. C., and Hartmann, L. 1987, *Ap. J.*, **316**, 323.
Innes, D.E., Giddings, J.R., and Falle, S.A.E.G. 1987, *M.N.R.A.S.*, **224**, 179.

Raga, A.C. 1988, *Ap. J.*, **335**, 820.
Raymond, J.C. 1979, *Ap. J. Suppl.*, **39**, 1.
Raymond, J.C., Hartigan, P., and Hartmann, L. 1988, *Ap. J.*, **326**, 323.
Reipurth, B. 1989a, *Nature* **340**, *42*.
Reipurth, B. 1989b, in ESO Workshop on *Low Mass Star Formation and Pre-Main Sequence Objects*, ed. Bo Reipurth (Garching : ESO), p. 247.
Reipurth, B., Bally, J., Graham, J.A., Lane, A.P., and Zealy, W.J. 1986, *Astr. and Ap.*, **164**, 51.
Reipurth, B., Raga, A.C., and Heathcote, S. 1991 (in preparation).
Solf, J. Böhm, K.H., and Raga, A.C. 1988, *Ap. J.*, **334**, 229.
Schwartz, R.D. 1975, *Ap. J.*, **195**, 631.
Schwartz, R.D. 1981, *Ap. J.*, **243**, 197.

L. Binette: Canadian Institute for Theoretical Astrophysics, 60 St. George Street, Toronto, Ontario M5S 1A1, Canada.
A.C. Raga: Department of Astronomy, The University, Manchester M13 9PL, U.K.